

## Field and petrographic data of 1.90 to 1.88 Ga I- and A-type granitoids from the central region of the Amazonian Craton, NE Amazonas State, Brazil

*Cristóvão da Silva Valério<sup>1\*</sup>, Moacir José Buenano Macambira<sup>2</sup>, Valmir da Silva Souza<sup>3</sup>*

**ABSTRACT** The SW Presidente Figueiredo district, which is located in the northeastern Amazonas State of the central Amazonian Craton, Brazil, consists of 1890 to 1898 Ma I-type granitoids (Terra Preta Granite, Água Branca Suite), A-type hornblende-bearing syenogranites (Canoas Syenogranite, Mapuera Suite), felsic to intermediate volcanic rocks (Iricoumé Group), and 1883 to 1889 Ma rapakivi granites (São Gabriel Granite, Mapuera Suite) and related rocks (quartz-gabbro-anorthosite and diorite), in addition to Castanhal quartz-monzonite, mylonites, and hornfels. The quartz-diorite facies of Terra Preta Granite were formed by mingling processes between a synplutonic quartz-gabbro dike and a hornblende granodiorite. Partially assimilated globules of Canoas hornblende-bearing syenogranite and their clear contacts with Terra Preta hornblende granodiorite suggest that Canoas Syenogranite is slightly younger than Terra Preta Granite. Canoas Syenogranite xenoliths inside São Gabriel Granite show that the granite is younger than the Canoas Syenogranite. New geologic and petrographic evidence improve the petrological understanding of these rocks and suggest that, in addition to fractional crystallization, assimilation and magma mingling played a role, at least at the local scale, in the evolution and compositional variation of the plutons. Such evidence is found in Terra Preta Granite mingled quartz-diorite, felsic material associated with the Canoas Syenogranite and in the intermediate microgranular enclaves, which exhibit primary biotite in hornblende-bearing rocks, plagioclase dissolution, corrosion of feldspars rims, alkali feldspar mantles, second apatite generation, and high xenocrystal contents in intermediate enclaves formed from the fragmentation of mafic intrusions. Petrographic analyses show that a deformational event recorded in the western part of the study area (with progressive deformation from E to W) is dated between the 1.90 Ga postcollisional magmatism and the intrusions of the São Gabriel Granite and related mafic/intermediate rocks (intra-plate). However, it is extremely necessary to obtain absolute ages for this metamorphic event.

*Keywords:* field data; petrography; I- and A- type granitoids; lithostratigraphy; NE Amazonas State.

**RESUMO** Dados de campo e petrográficos de granitoides dos tipos I e A de 1,90 a 1,88 Ga da região central do Cráton amazônico, NE do Estado do Amazonas, Brasil. O SW do município de Presidente Figueiredo, localizado no Estado do Amazonas, Nordeste do Cráton Amazônico Central, Brasil, hospeda granitoides do tipo I de idade entre 1890 a 1898 Ma (Terra Preta Granito, Suíte Água Branca), hornblenda-sienogranitos do tipo A (Sienogranito Canoas da Suíte Mapuera), rochas vulcânicas ácidas à intermediárias (Grupo Iricoumé) e granitos rapakivi de idades entre 1883 a 1889 Ma (Granito São Gabriel da Suíte Mapuera), e rochas afins (quartzo-gabro-anortosito e diorito), além de quartzo-monzonito Castanhal, milonitos e hornfels. A fácies quartzo-diorito do granito Terra Preta foi formada por processos de mistura entre um dique quartzo-gabro sinplutônico e um granodiorito hornblenda. Glóbulos parcialmente assimilados de sienogranitos hornblenda Canoas e seus contatos com o granodiorito hornblenda Terra Preta sugerem que o sienogranito Canoas é um pouco mais jovem do que o Granito Terra Preta. Xenólitos do sienogranito Canoas no interior do Granito São Gabriel mostram que o granito é mais jovem do que o sienogranito Canoas. Novas evidências geológicas e petrográficas avançam na compreensão petrológica destas rochas e sugerem que, além de cristalização fracionada, assimilação e mistura de magma, desempenharam um papel importante, pelo menos em escala local, na evolução e variação composicionais dos plutons. Tal evidência é encontrada no Granito Terra Preta misturado com materiais quartzo-diorito, fêlsico associado ao sienogranito Canoas e nos enclaves microgranulares intermediários, que apresentam biotita e hornblenda primárias, além de dissolução plagioclásio, corrosão de feldspatos, mantos feldspatos alcalinos, segunda geração de apatita, e elevados teores xenocristais em enclaves intermediários formados a partir da fragmentação de intrusões máficas. Análises petrográficas mostram que um evento deformacional registrado na parte Ocidental da área de estudo (com deformação progressiva de E para W) é estimado entre o magmatismo pós-colisional de 1,90 Ga e as invasões do Granito São Gabriel e rochas afins máficas/intermediárias (intraplaca). No entanto, torna-se extremamente necessário obter idades absolutas para este evento metamórfico.

*Palavras-chave:* dados de campo; petrografia; granitoides dos tipos I e A; litoestratigrafia; NE do Estado do Amazonas.

<sup>1</sup>Geosciences Institute, Federal University of Roraima, Boa Vista (RR), Brazil. E-mail: cristovao@igeo.ufr.br

<sup>2</sup>Laboratory of Isotope Geology, Geosciences Institute, Federal University of Pará, Belém (PA), Brazil. E-mail: moamac@ufpa.br

<sup>3</sup>Geosciences Institute, University of Brasília, Brasília (DF), Brazil. E-mail: vsouza@unb.br

\*Corresponding author

**INTRODUCTION** The igneous associations in the northeastern Amazonas State, southern Uatumã-Anauá domain, are generically included in regional units based on limited knowledge of their field relationships and petrography. Recently, new outcrops of granitoids and related rocks, in addition to granitoids that recorded subsolidus deformation, were found. These rocks and their contact relationships revealed important information that allowed updating the lithostratigraphy of the southern Uatumã-Anauá domain. Moreover, detailed field and petrographic studies showed the first insights on the dynamic processes involved in the generation of the granitoid facies, and a new tectonic interpretation based on micro-deformational analysis was proposed.

In spite of modern methodologies advance, classic methods still supply enough information for understanding of the geology of remote areas. These methods are fundamental in areas in which the geological history is poorly understood, such as in the central Amazonian craton.

The objectives of this study were: presenting an integrated geological map, proposing a new lithostratigraphy for rocks of the southern region of the Uatumã-Anauá domain, discussing petrological and deformational features, and summarizing new data on the field of relationships and petrography of the 1.90 to 1.88 Ga I- and A-type granitoids and related rocks from the south portion of the Uatumã-Anauá domain in the central Amazonian craton, Brazil.

**GEOLOGICAL SETTING** Tassinari & Macambira (1999 and 2004) and Tassinari *et al.* (2000) subdivided the Amazonian Craton into Central Amazon (> 2.3 Ga), Maroni-Itacaiunas (2.2 – 1.95 Ga), Ventuari-Tapajós (1.95 – 1.8 Ga), Rio Negro-Juruena (1.8 – 1.55 Ga), Rondoniana-San Ignacio (1.5 – 1.3 Ga), and Sunsás (1.25 – 1.0 Ga) geotectonic provinces (Fig. 1A). Based on this model, this study was carried out in the central portion of the Ventuari-Tapajós Province, central Amazonian Craton, in the Uatumã-Anauá domain (CPRM 2006, Almeida 2006, Almeida *et al.* 2008).

The Uatumã-Anauá domain has rocks from the entire Orosirian period, mainly composed of igneous units, in addition to Paleoproterozoic and Phanerozoic sedimentary cover that filled the Amazonas basin, as seen in Fig. 1B (CPRM 2000 & 2006, Faria *et al.* 2003, Ferron 2006, Valério 2006, Almeida 2006). Early regional mapping carried out

in this region identified several felsic and mafic igneous rocks (Santos *et al.* 1974, Araújo Neto & Moreira 1976, Veiga Jr. *et al.* 1979, Costi *et al.* 1984). Later studies have focused on the petrography, geochemistry, and geochronology of felsic to intermediate granitoids and volcanic rocks (Valério *et al.* 2005, 2006 A & B 2009, & 2010, Souza *et al.* 2006, Marques *et al.* 2007, Souza *et al.* 2007, Freitas *et al.* 2007, Souza & Nogueira 2009, Costi *et al.* 2009).

The country rock of the Uatumã-Anauá domain consists of tonalite-trondhjemite-granodiorite (TTG)-like calc-alkaline meta-granitoids of the Anauá Complex (2.03 Ga) in association with meta-volcanic sedimentary rocks of the Uai-Uai Group (1.97 Ga?), both representing volcanic arc and back-arc basin settings (Faria *et al.* 2002 & 2003). According to Almeida (2006) and Almeida & Macambira (2007), the Anauá basement was intruded by S- (Serra Dourada, 1.96 Ga) and I-types (Matins Pereira, 1.97 Ga), and calc-alkaline granitoids in a collisional setting.

The youngest igneous rocks of the Uatumã-Anauá domain are 1.89 to 1.90 Ga I-type, high-K calc-alkaline granitoids of the Água Branca Suite, felsic to intermediate volcanic rocks of the Iricoumé Group, A-type granites of the Mapuera Suite (1.87 to 1.89 Ga, Abonari and São Gabriel granites), and related rocks (quartz-gabbro, diorite and minor anorthosite), in addition to quartz-monzonites, mylonites and hornfels (Valério *et al.* 2009 & 2010 and Costi *et al.* 2009). According to Santos *et al.* (2001 and 2006), the Mapuera granites are also associated with 1.87 Ga charnockites. After the first generation of the Mapuera A-type granites and a gap of ca. 60 Ma, a second generation of tin-bearing, A-type, anorogenic granites (1.81 Ga) of the Madeira Suite intruded in the Pitinga region (Costi *et al.* 2000). These latter have a similar age to the Moderna Granite in northernmost Brazil (Santos *et al.* 1997). In addition to the youngest units, metagranites, metamafics and gneiss in the southern portion of the Guyana Shield have been grouped into Jauaperi complex (CPRM 2006).

**IGNEOUS ASSOCIATIONS** The study area consists of I-type, high-K calc-alkaline granitoids of the Terra Preta Granite (Água Branca Suite), volcanic and pyroclastic rocks (Iricoumé Group), A-type hornblende-bearing syenogranites of the Canoas Syenogranite (Mapuera Suite), rapakivi granites of the São Gabriel Granite (Mapuera Suite), and

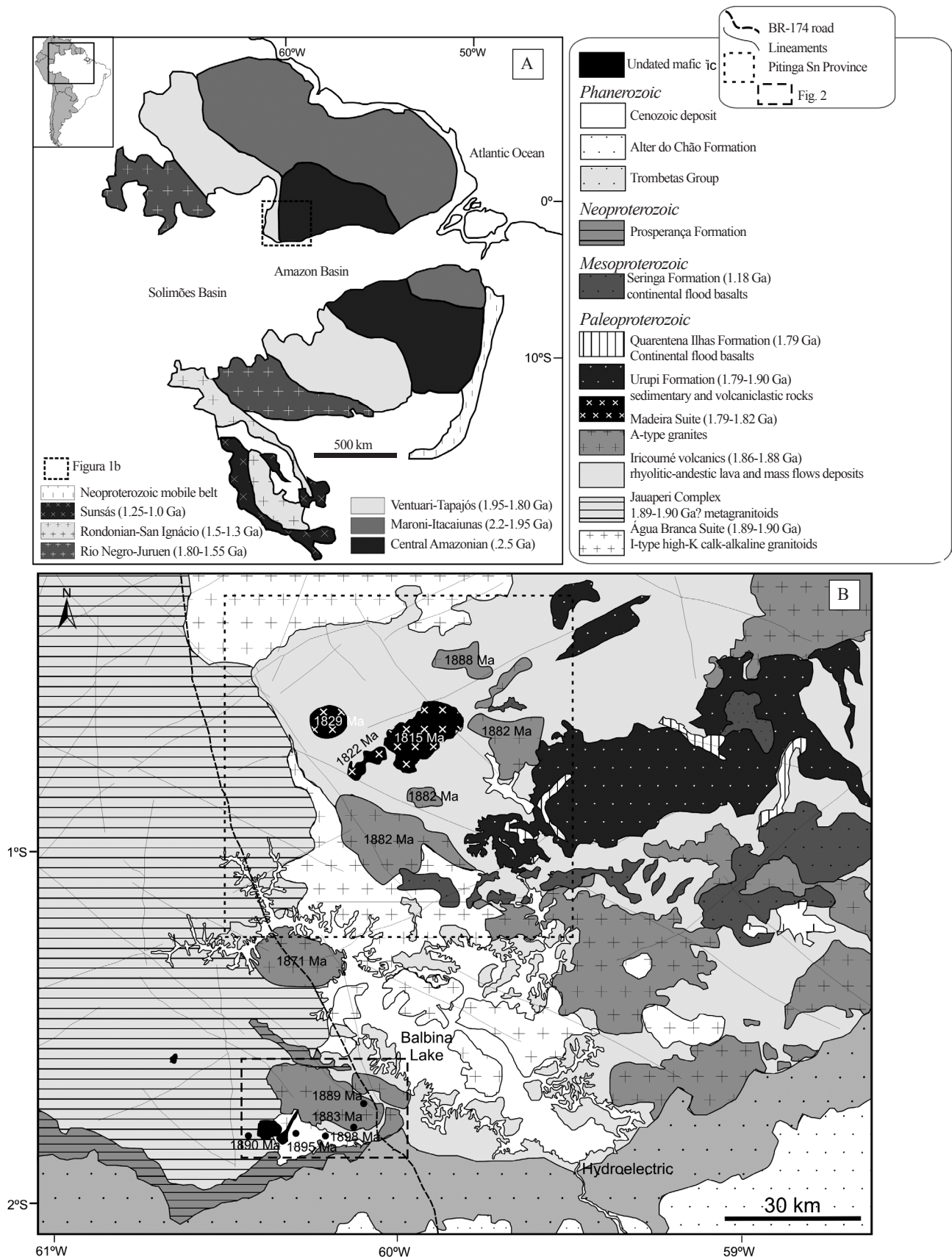


Figure 1 – (A) Tectonic provinces of the Amazonian Craton (Tassinari and Macambira 1999, modified by Macambira et al. 2009); (B) simplified geological map of the central Amazonian Craton, NE Amazonas State (modified from CPRM 2006, Ferron et al. 2006, and Valério et al. 2006b and 2009).

Castanhã quartz-monzonite. The area also includes mafic dikes associated with granitoids, younger mafic

stocks and dikes likely belonging to the Seringa and/or Quarentena Ilhas formations. Some of the granitoids

display features of dynamo-static crystallization and static re-crystallization (thermal metamorphism), probably linked to shear zones and mafic intrusions, which have not yet been well characterized (Fig. 2).

**Terra Preta Granite** The size and shape of the Terra Preta Granite remain undefined due to reworking of its western and southern borders caused by a poorly defined deformational event, and the cover of the Amazon basin. Its compositional variation consists on quartz-diorite (mingled), hornblende monzodiorite, hornblende tonalite, hornblende granodiorite, biotite-hornblende granodiorite, hornblende monzogranite, biotite-hornblende monzogranite, biotite monzogranite, and biotite syenogranite.

Terra Preta Granite hosts aplite, mafic and intermediate dikes, and enclaves. The contacts of the aplite dikes with the wall rock are sharp and have no chilled borders. The granite has two types of enclaves: volcanic xenoliths and mafic and intermediate microgranular enclaves. The xenoliths of glomeroporphyritic andesite have sub-rounded shapes and their contacts with the wall rock are abrupt, irregular and lack chilled borders. The mafic enclaves are circular to ellipsoidal, with 5 to 40 cm in diameter or length and display a mesocratic color-index, irregular transitional contacts and a high content of wall rock crystals (feldspars and quartz xenocrysts). Another important feature is a NE-striking gabbro dike that intruded into the contact between the Terra Preta

Granite and Canoas Syenogranite (Fig. 3A). Radar imagery shows that the southern part of the dike was inflected to strike NW-SE. The contact of the dike with the Terra Preta hornblende granodiorite is characterized by the formation of a transitional zone containing features of magma mingling (Fig. 3B), as well as dike fragmentation and formation of sub-angular to rounded microgranular enclaves and a mingled rock (quartz-diorite), as observed in Fig. 3C. Such aspects indicate a synplutonic dike that was partially fragmented and that physically and chemically interacted with the granodioritic magma before completely chilling.

**Iricoumé Group** The rocks of the Iricoumé Group include pyroclastic flows (eutaxitic ignimbrite, ignimbrite, and co-ignimbrite), lava flow (andesite/traquiandesite and rhyolite/rhyodacite) deposits, and intrusions of autoclastic breccias. The lithostratigraphic sequence shows alternations of lava flow deposits above fiamme-rich ignimbrites, followed by ignimbrites and co-ignimbrites.

The basis of the mass flow deposits is formed by ignimbrites with highly flattened pumices (fiammes), and crystal and lithic fragments characterized by eutaxitic textures. Its origin, at least in the ignimbrites, was the welding compaction of pumice clasts (Bull & McPhie 2007). The ignimbrites/co-ignimbrites display fragmentary textures and a fine matrix, layers with gradational fining upward cycles



Figure 2 – Geological map of the southwestern Presidente Figueiredo district, NE Amazonas State, central Amazonian Craton. The boundaries of the granitoid and volcanic facies and main fault zones have been estimated from the integration of field data, SAR/SIPAM remote sensing products, and airborne geophysical data.

containing  $\leq 20$  cm ejected fragments (bombs), and gas escape-related vesicular cavities between the layer boundaries.

The andesites/traquiandesites display several amygdaloidal cavities related to gas release. The presence of autoclastic breccias suggests an emplacement similar to cauldron collapse. The breccias have a rhyolite-rhyodacite matrix and are composed of highly varied rock fragments of andesite, rhyolite, and pumice.

**Canoas Syenogranite** The Canoas Syenogranite consists of a group of ellipsoidal NW-SE stocks with 5 to 15 km length, mainly composed of reddish syenogranite and minor alkali feldspar-granite (Fig. 2). It has two types of contacts with the Terra Preta Granite. The intrusions measuring less than 5 km in diameter generated outward and inward aureoles. The outward aureole is characterized by a thick alteration zone ( $> 1$  m) marked by a color change likely caused by low temperature of aqueous fluids. The narrow inward aureole ( $< 20$  cm) is characterized by increasing grain size and quartz content, and it is likely recrystallized. The fine-grained stock borders reflect rapid heat loss to the wall rock that characterizes chilled borders. The contact between a large stock ( $> 15$  km length) and the wall rock (Terra Preta hornblende granodiorite) is interdigitated, and chilled borders were not observed. The presence of rounded globules of syenogranite assimilated by granodioritic magma and the contact type suggest physical interaction between both magmas before complete crystallization. Therefore, it is plausible that the Canoas Syenogranite is slightly younger than the Terra Preta Granite. The mafic enclaves of the Canoas Syenogranite are circular, with part of their ellipsoidal shape preserved, and the contacts with the wall rock are irregular and show strong assimilation.

Quartz-gabbro dikes oriented WNW-ESE/ $70^{\circ}$ SW are the main features that indicate magma mingling processes. The features include fracturing and fragmentation of the dike borders (8 to 15 cm angular and  $< 5$  cm rounded fragments), with the formation of mingled material among the mafic fragments. The irregular and interdigitated contact with the wall rock is marked by a narrow transitional zone ( $\sim 5$  cm) containing  $< 1$  cm rounded mafic enclaves (Fig. 3D). The contact presents evidence of thermal contrast and interaction between the dike and the wall rock, whereas the small rounded enclaves

reveal extensive interaction between both felsic and mafic systems.

**São Gabriel Granite** Rapakivi-type hornblende monzogranite, hornblende syenogranite, and biotite-hornblende syenogranite are the major petrographic variations observed in São Gabriel Granite. Microgranite porphyry and microdiorite occur infrequently as dikes near the boundaries of the batholith.

The São Gabriel Granite is an irregular, NW-SE striking, sub-ellipsoidal-shaped pluton (Fig. 2). Its main field features include volcanic, granitic and mafic enclaves, in addition to mafic and intermediate dikes. The volcanic xenoliths are sub-rounded and present dacitic compositions. The borders of the enclaves are irregular, sharp, and composed of imbricated quartz and feldspars crystals. The eastern and southeastern borders of the granite are characterized by sub-angular xenoliths of recrystallized alkali feldspar-rich syenogranites (muscovite-actinolite hornfels), likely from the Canoas Syenogranite, whose contacts with the wall rock vary from straight and abrupt to irregular ones (Fig. 3E).

The presence of these xenoliths demonstrates that the Canoas stocks are slightly older than the São Gabriel Granite. The textural dissimilarity between the preserved Canoas plutons (granoblastic) and the sub-angular xenoliths (granolepidoblastic) suggests that these fragments, which are partially assimilated by São Gabriel magma, preserved the effects of a dynamo-thermal deformation event, which was followed by a mafic intrusion-related thermal event. Alternatively, the foliation of xenoliths could have been caused by the increasing turbulent flux close to the borders of the São Gabriel magma chamber.

The contact between the biotite-hornblende syenogranite and the microgranite porphyry is clear (Fig. 3F). In general, the São Gabriel mafic enclaves are sub-rounded and include high contents of xenocrystals from the host rock. Along the granite pluton boundaries, they are stretched according to the igneous foliation. Mafic dikes that fill fractures in the São Gabriel Granite do not have features that support a genetic correlation. However, the intermediate dikes were frequently linked to all petrographic types.

**Mafic and intermediate intrusions** The dikes and stocks of the gabbros, diorites and anorthosites are associated with each other according to geographic criteria and petrographic similarities (segregation

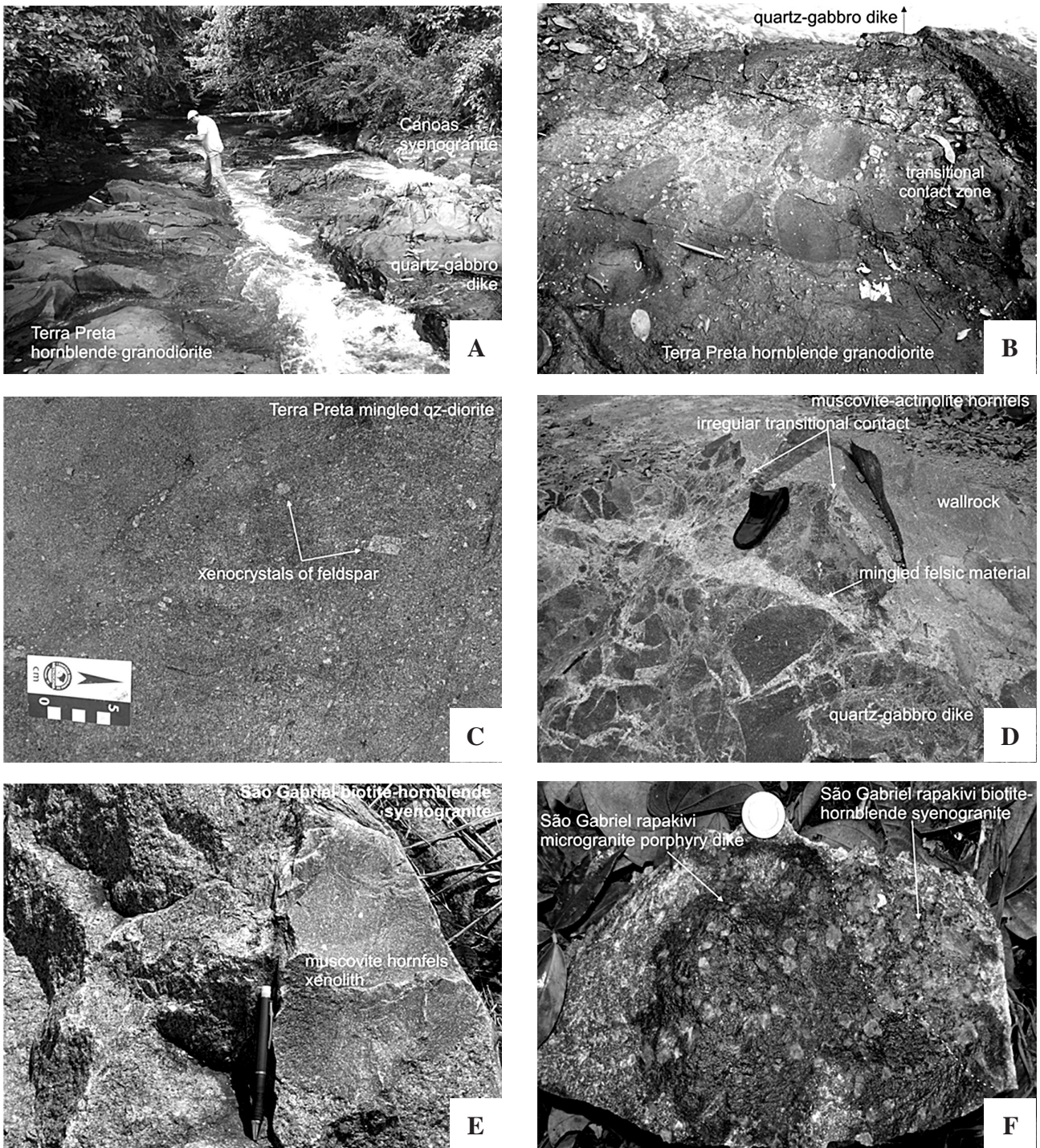


Figure 3 – Field features of the Terra Preta, Canoas and São Gabriel granitoids and related rocks. (A) Quartz-gabbro dike emplacement into the contact zone between Terra Preta hornblende granodiorite and Canoas syenogranite; (B) zone of transitional contact between a quartz-gabbro dike and Terra Preta hornblende granodiorite, showing fragmentation and mingling of the dike, and subangular to rounded mafic enclaves without visible xenocrysts (dropped crystals); (C) Terra Preta mingled quartz-diorite with variable feldspar xenocrysts; (D) contact between a mafic dike and wallrock (muscovite-actinolite hornfels). Arrows show the formation of mingled material among the incompletely crystallized mafic fragments and a narrow (~ 5 cm) transitional zone. (E) Sub-angular xenoliths of recrystallized syenogranite (muscovite-actinolite hornfels) of Canoas Syenogranite inside São Gabriel Granite; (F) regular contact between biotite-hornblende syenogranite and microgranite porphyry dike.

and fractionation) as it was elsewhere observed (Campbell 1996). In the field, the intrusions did not display clear relationships with the wall rocks, and

the outcrops are restricted to blocks and flagstones located along tracks and small creeks. The rocks are often very weathered.

## PETROGRAPHY

**Material and methods** The petrographic analysis consisted on the microscopic characterization of 165 polished thin sections that represent the compositional variations and geographical distribution of the rocks from the study area. The classification of granitoid varieties and enclaves, totalizing 62 samples, was based on the modal parameters obtained by counting 1,500 points for medium- and fine-grained rocks and 1,800 for coarse-grained types. The composition of plagioclase zones was obtained from the Michel-Lévy conventional method and, when possible, from the 010 cleavage-Albite Law twinning and Albite Law-Carlsbad twinning methods (variations of the Michel-Lévy method), as described by Hibbard (1995).

**Terra Preta Granite** According to their mineralogical compositions, the main facies observed in the Terra Preta Granite are hornblende monzodiorite, hornblende tonalite, hornblende granodiorite, hornblende-biotite granodiorite, hornblende monzogranite, hornblende-biotite monzogranite, and biotite syenogranite, besides the mingled quartz-diorite (Tab. 1, Fig. 4A). The main texture is seriate but it varies to porphyritic, fine-grained equigranular and, locally, to granophyric.

Two types of plagioclase, both euhedral, were identified. Plagioclase-1 measures 1.5 to 4.0 mm and varies from  $An_{22-21}$  in the core to  $An_{25-22}$  in the rims. Progressive oscillatory zoning is common, whereas sudden oscillatory zoning is rare. Apatite and zircon inclusions are common in the core and rims, whereas Fe-Ti oxides inclusions only happen in the rims. Plagioclase-2 (< 0.5 mm) is usually zoned, and its composition varies from  $An_{28}$  in the core to  $An_{22-25}$  in the rim. In both types, the contacts with all other minerals are straight (Tab. 2).

Three types of quartz were identified. Quartz-1 is sub-hedral – anhedral ( $\leq 1$  mm) and has opaque titanite and hornblende inclusions. Quartz-2 is associated with alkali feldspar-2 to form magmatic granophyric textures in the granodiorites. Quartz-3 is a hydrothermal phase that was precipitated on the alkali feldspar-1.

Three types of alkali feldspar were identified: alkali feldspar-1 is euhedral and measures from 2 to 8 mm in length. Film-, strings- and interlocking-type perthites are common. In the monzogranite, the insular perthite surrounds perthitic alkali feldspar, whereas the albite chessboard is developed in the syenogranites. A second-generation of perthite (flames-type) is linked

to subsequent deformation processes. In the contacts with alkali feldspar, it developed a swapped rim structure related to albite intergranular migration caused by Na-K exchange (Smith & Brown 1988). Alkali feldspar-2 represents those portions of the granophyric textures of the granodiorites. The anhedral alkali feldspar-3 (0.5 – 2.0 mm) has planar contacts with quartz 1 and -2 and interpenetrative contacts with quartz 3. Interlocking and flame perthites are frequent, whereas the beads-type one occurs locally. Apatite and zircon inclusions are common in this mineral. In the porphyry portion of the granodiorite, alkali feldspar-3 exhibits strings, veins, microfilms and recrystallization-linked flame perthites.

The hornblende is euhedral and sub-hedral and displays planar contacts with the quartz and alkali feldspar and interpenetrative contacts with the titanite. Fe-Ti oxides, zircon and apatite inclusions are very common. In the alkali feldspar-poor petrographic types, hornblende also occurs as a product of an early reaction between the liquidus and clinopyroxenes, forming clinopyroxene pseudomorphs.

Sub-hedral biotite-1 has hornblende, Fe-Ti oxides and titanite inclusions, while biotite-2 occurs as anhedral interstitial crystals associated with titanite.

The Fe-Ti oxides occur both associated with varietal minerals and as inclusions. The titanite is euhedral and is commonly associated with varietals. The apatite needles are euhedral–sub-hedral and measure < 0.1 mm. In the granodiorites, apatite crystals grew up to 2 mm (type-2 apatite). The zircons are euhedral–sub-hedral and zoned, and they always happen in association with apatite.

The epidote is originated from more calcic portions of plagioclase and hornblende. The sericite-muscovite and argilic minerals commonly occur on alkali feldspar and less commonly on plagioclase. The intergranular albite and individual crystals are associated with exsolution of the sodic phase from alkali feldspar to form perthites. The actinolite appears as individual crystals and rims of hornblende and clinopyroxene pseudomorphs.

**MAFIC DIKES AND ENCLAVES** The gabbro dikes and related mafic enclaves (sub-angular) possess intergranular textures and high clinopyroxene pseudomorph contents. Despite being intensely decalcified, some measurements of plagioclase revealed calcic andesine compositions ( $An_{41-48}$ ). The sub-hedral calcic andesine contains inclusions of



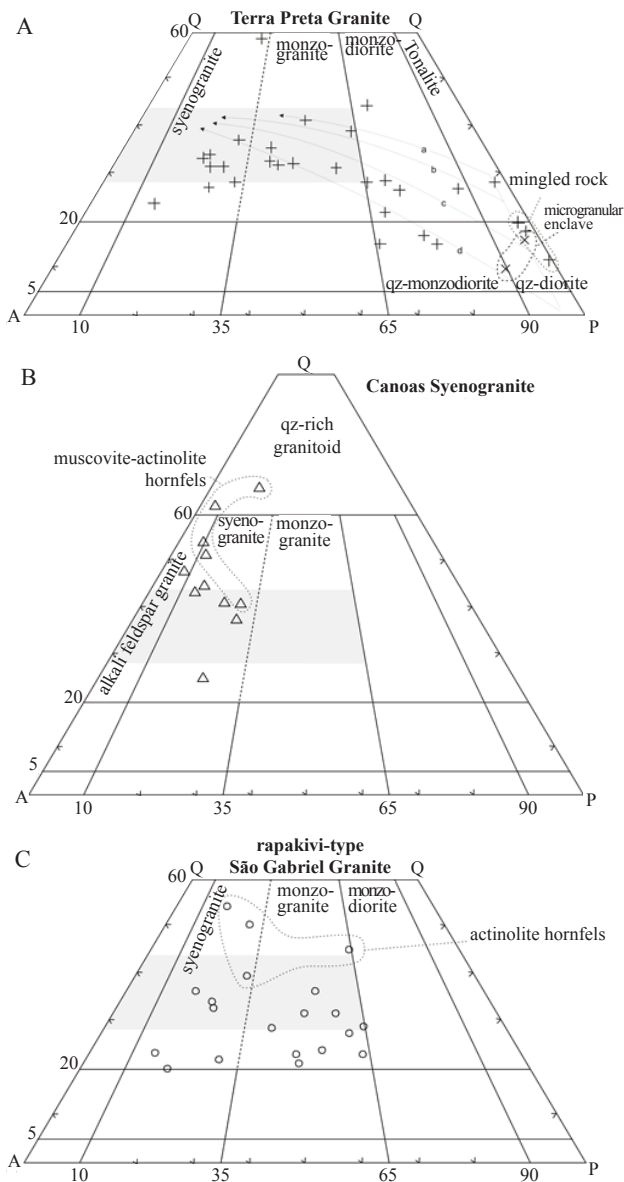


Figure 4 – QAP modal composition of the studied plutons (Streckeisen 1976). Granitic series according to Lameyre and Bowden (1982). (A–C) calc-alkaline granodioritic subseries (A – Corsica, Sardinia; B – Chile, C – Peru). The dashed field corresponds to granites generated from crustal melting, according to Lameyre & Bowden (1982).

Fe-Ti oxides and displays interpenetrative contacts with hornblende. Actinolite and chlorite are the products for the substitution of clinopyroxene and hornblende, respectively. They are usually fibrous and include Fe-Ti oxide inclusions when altered to biotite (Tab. 3). The dikes have rounded clasts filled by fine-grained tremolite-actinolite and subordinate plagioclase. Their rims are formed by fibrous crystals ( $\leq 1$  mm) of tremolite-actinolite that display sutured contacts with the host rock (Fig. 5A). The absence of inclusions, granulation, and contact type suggest that the mineral clasts are a late crystallized vesicular

phase filled by secondary minerals (amygdales), suggesting near-surface chilling.

#### MINGLED QUARTZ-DIORITE AND RELATED ENCLAVES

The mingled quartz-diorite displays intergranular textures and a mineralogical assemblage formed by poikilitic crystals of quartz and alkali feldspar (string and flames perthites), xenocrysts of quartz, plagioclase and alkali feldspar, plagioclase, hornblende, high titanite content Fe-Ti oxides, apatite, zircon, and actinolite. The poikilitic crystals include hornblende, plagioclase, and titanite inclusions. All xenocrysts from the wallrock exhibit re-absorption/re-equilibrium features (engulfing, corroded core and patchy zones) (Fig. 5B). The preserved mafic phase possesses two types of plagioclase, both of which are intensely altered. The 1-type (from 2 to 3 mm) has a euhedral habit and oscillatory zoning with preserved sodic rims. It contains Fe-Ti oxides, apatite and zircon inclusions in the core and hornblende in the rims, and sharp contacts with other minerals except hornblende, which have interpenetrative contacts. Plagioclase-2 is sub-hedral ( $< 1$  mm) and is frequently associated with hornblende. Hornblende-1 is euhedral-sub-hedral with Fe-Ti oxides and titanite inclusions. This hornblende has interpenetrative contacts with plagioclase-1 and straight contacts with quartz and alkali feldspar. Hornblende-2, quartz and alkali feldspar are interstitial. Two types of apatite were also identified: a long/narrow (20:1) and a short/wide (5:1).

#### Iricoumé Group

**PYROCLASTIC FLOW DEPOSITS** Lithic fragments and bent fiamme lenses make up the eutaxitic or fiamme-rich ignimbrite. The lithic clasts are angular and very fragmented. The fiammes show wrinkled rims and are locally smooth. The ash matrix has an accentuated orientation and high degree of welding by compaction. The ignimbrite exhibits a microlithic texture and strong mineral foliation or orientation from pyroclastic flow. The ignimbrite is composed of fragments of quartz, alkali feldspar, plagioclase, biotite and Fe-Ti oxides, pumice fragments, and fine-grained ash matrix. The co-ignimbrite consists of similar proportions of clasts of quartz, alkali feldspar, plagioclase and opaques, as well as ash matrix.

**LAVA FLOW DEPOSITS** The andesite has a glomeroporphyritic amygdaloidal texture and consists of phenocrysts of quartz, calcic oligoclase ( $An_{22-25}$ ), pyroxene and hornblende in a trachytic matrix, with

Table 2 – Petrographic characteristics of studied granitic plutons

Pluton, Unit	Terra Preta Granite, <i>Água Branca Suite</i>	Canoas Syenogranite, <i>Mapuera Suite</i>	São Gabriel Granite, <i>Mapuera Suite</i>
Petrographic variation	(Hornblende)quartz-diorite, monzodiorite, tonalite, granodiorite, and (biotite)monzogranite and -syenogranite.	Hornblende-bearing syenogranite and alkali feldspar granite.	Hornblende monzogranite, hornblende syenogranite, biotite-hornblende syenogranite.
Textural variation	The seriate texture varies to porphyritic, fine-grained equigranular and localized granophyric textures.	Medium- to fine-grained seriate texture.	Medium- to coarse-grained seriate texture.
<i>Essential minerals</i>			
Plagioclase-1	Length 1.5–4.0 mm, calcic oligoclase (An <sub>22-21</sub> in core), (An <sub>25-22</sub> in rims), progressive oscillatory zoning, apatite and zircon inclusions are common in core and rims, Fe-Ti oxides inclusions only in rims, contacts with all others minerals are rectilinear.	Euhedral, 0.5–3.0 mm, unzoning, sodic oligoclase (An <sub>10-12</sub> ), twinning Albite and Albite-Carlsbad Laws. Its contact with the alkali feldspar and quartz is rectilinear and with hornblende is interdigitated.	Euhedral (2–6.5 mm), An <sub>22</sub> -An <sub>28</sub> in core, An <sub>22-17</sub> in rims, contact is rectilinear with the hornblende-1 and interpenetrative with the quartz-1, contains hornblende-Fe-Ti oxides, apatite and zircon inclusions. Twinning Albite and Albite-Carlsbad Laws and major normal zonings, and abrupt and sectorized oscillatory zonings.
Plagioclase-2	< 0.5 mm, indefinite zoning, An <sub>28</sub> in core and An <sub>22-25</sub> in rims, contacts with all others minerals are rectilinear.	absent phase	0.5–1.5 mm, anhedral-subhedral, abrupt oscillatory zoning. Occurs filling in interstices among grains and contains inclusions of quartz-1 and biotite-2, An <sub>27-25</sub> in core and An <sub>21-17</sub> in rims, alteration to epidote and sericite in calcic zone.
Alkali feldspar-1	Euhedral, length 2–8 mm. Film-, strings- and interlocking-type perthite are common. In monzogranites, the insular perthite occurs surrounding perthitic alkali feldspar, albite-chessboard developed in syenogranites. A perthite second-generation (flames-type) is linked to subsequent deformation processes. In contacts with others alkali feldspar developed swapped rims.	Subhedral, strongly perthitic (stringlets, strings, interlocking and chessboard albite) with generation of subhedral crystals of albite. It possesses several plagioclase inclusions and its contact with the plagioclase and quartz is faintly interdigitated.	Subhedral, 2.5–6.0 mm, commonly occurs associated to the quartz-1, local interlocking and beads perthites, albite intergranular occur, corroded rims form ovoid shape (rapakivi texture). Both alkali feldspar present Albite-Pericline Law twinning, slightly transformed to sericite and argilic minerals, contain plagioclase-2, hornblende-1, zircon and apatite as inclusions and albite microfilms and string perthite are very common.
Alkali feldspar-2	Anedral, 0.5–2.0 mm, rectilinear contact with the quartz-1 and -2 and interpenetrative with the quartz-3.	absent phase	It is subhedral-anhedral, measures 0.5–2.5 mm.
Quartz-1	Subedral-aneedral ( $\leq 1$ mm), titanite, opaques and hornblende inclusions.	Anedral and contains titanite and opaques inclusions	Anhedral-subhedral, 1–1.5 mm.
Quartz-2	Alkali feldspar-2-associated to form a magmatic granophyric texture.	absent phase	Interstitial, occurs associated to the biotite-2.
Quartz-3	Represents a hydrothermal phase precipitated on the alkali feldspar-1.	absent phase	It shows strongly undulatory extinction, typically occurs included in the alkali feldspar-1.

Continua...

Table 2 – Continuation

<i>Varietal minerals</i>	
Hornblende-1	<p>Euhedral–subhedral, rectum contact with quartz and alkali feldspar and interpenetrative with the titanite. Fe-Ti oxides, zircon and apatite inclusions are very frequent. It also occurs as clinopyroxene pseudomorphs.</p> <p>Strongly altered to chlorite, occurs commonly as interstitial crystals containing inclusions of Fe-Ti oxides.</p> <p>Subhedral to euhedral. It is associated to F-Ti oxides titanite, alteration to chlorite, epidote and biotite. The contact with the plagioclase-1 is rectilinear and with the quartz-1 and alkali feldspar-1 is interdigitated. Contains inclusions of Fe-Ti oxides.</p>
Hornblende-2	<p>absent phase</p> <p>associated to quartz-2, occurs filling in interstitials and mainly cleavages of plagioclases</p>
Biotite-1	<p>Subedral, contains hornblende, Fe-Ti oxides and titanite as inclusions.</p> <p>absent phase</p> <p>Subhedral, contains several corroded magnetite and ilmenite inclusions.</p>
Biotite-2	<p>Occurs as anhedral interstitial crystals and titanite-associated.</p> <p>absent phase</p> <p>Occurs as product of transformation of hornblendes and as filling in interstices.</p>
<i>Accessory minerals</i>	
Fe-Ti oxides	<p>Occur associated to varietals and as inclusions.</p> <p>mischaracterized</p> <p>They combine with Fe-Mg hydrated minerals and titanite.</p>
Titanite	<p>Euhedral, occurs commonly associated to varietals.</p> <p>Some crystals have been altered to epidote</p>
Apatite-1	<p>Apatite needles are euhedral–subhedral and measure &lt; 0.1 mm.</p> <p>mischaracterized</p> <p>Euhedral, acicular and hexagonal, and exhibits intimate relations with the hornblende-2 and plagioclases.</p>
Apatite-2	<p>Crystals grew up to 2 mm.</p> <p>absent phase</p> <p>absent phase</p>
Zircon	<p>Euhedral–subhedral, zoned, always occurs associated to apatite.</p> <p>Euhedral–subhedral and sharply zoned.</p>
Garnet	<p>absent phase</p> <p>absent phase</p>
<i>Secondary minerals</i>	
Epidote	<p>Originated from more calcic portions of plagioclase and hornblende.</p> <p>From calcic portion of plagioclases.</p> <p>It stands out by forming euhedral crystals.</p>
Sericite-muscovite	<p>Majorly occur on alkali feldspar and plagioclase.</p> <p>From alkali feldspar and plagioclase.</p> <p>Occurs associated to calcic portions of plagioclases.</p>
Argillic minerals	<p>Occur on alkali feldspar and plagioclase.</p> <p>From alkali feldspar.</p> <p>The argillization occurred with small intensity in alkali feldspars.</p>
Intergranular albite	<p>Are associated to separation of the sodic phase from alkali feldspar to form perthites.</p> <p>From perthite and albite chessboard.</p> <p>It is product from the perthite.</p>
Actinolite	<p>Occurs as individual crystals and rims of hornblende and clinopyroxene pseudomorphs.</p> <p>From hornblende.</p> <p>absent phase</p>
Chlorite	<p>Occurs faintly from biotites.</p> <p>From hornblende.</p> <p>From hornblende and biotite.</p>
Hematite	<p>absent phase</p> <p>Occurs as impregnation on alkali feldspar, as filling into microfractures.</p> <p>Common in the alkali feldspar-rich granites, as impregnation in sodic lamellas of perthites, interstitial portions and microfractures and as espherulitic crystals.</p>

Table 3 – Main petrographic and mineralogical characteristics of rocks associated to appraised granitic plutons.

Pluton	Terra Preta Granite	Canoas Syenogranite	São Gabriel Granite
Felsic dike	Microsyenogranite, rhyolite with inequigranular and microporphyritic textures. Alkali feldspar phenocrystals are perthitic and presents Albite-Pericline Law twinning.		
Xenoliths	Glomeroporphyritic andesite with a very fine-grained matrix formed by clusters of amphiboles, feldspars and quartz. Two phenocrystals types of plagioclase: 1-type has 2–8 mm, $An_{2,4}$ in core and $An_{2,1}$ in rim; 2-type has < 0.5 mm, $An_{38}$ in core and $An_{26}$ in rim.		1. Muscovite-actinolite-hornfels (Canoas Syenogranite) with interlobate granoblastic texture. 2. Hornblende-rhyodacite.
Mafic dike	Intergranular texture gabbros and high clinopyroxene pseudomorphs content emphasize the gabbro dike and enclaves associated. subhedral calcic andesine ( $An_{41-49}$ ). It also is formed by circular fine-grained tremolite-actinolite crusts and subordinated plagioclase, whose rims are formed by fibrous crystals of tremolite-actinolite.	Shows intergranular and sub-ophitic textures, high amphiboles contents and plagioclase xenocrystals. The xenocrystals have been partially dissolved in their core and rims.	
Mafic enclave	Idem to mafic dike.		
Intermediate enclave	Quartz-diorite, intergranular texture, a mineralogical assembly formed by poikilitic crystals of quartz and alkali feldspar (string and flames perthites), xenocrystals of quartz, plagioclase and alkali feldspar, and, high titanite content. Xenocrystals exhibit engulfing, corroded core and patchy zone, and also possesses a mafic phase preserved and two apatite types, a long/narrow (20:1) and another short/wide (5:1).	Quartz-diorite kept petrographic features similar to Terra Preta mafic enclaves. Exceptions include the biotite presence, amphibole pseudomorphs and plagioclases lightly more calcic ( $An_{7,30}$ ).	
Metagranitoids	Dynamo-static deformation progressively increasing from E to W into the W sector of studied area. Its intensity embraces low, low-medium and medium-high temperature degrees.		
Iricoumé ignimbrite	Lithic fragments and bent fiammes constitute the fiamme-rich ignimbrite. It is formed by crystals fragments of quartz, alkali feldspar, plagioclase, biotite and Fe-Ti oxides, and pumice fragments and fine-grained ash matrix. The co-ignimbrite consists of similar proportions of clasts of quartz, alkali feldspar, plagioclase and opaques, besides ash matrix.		
Iricoumé andesite/trachyandesite	Glomeroporphyritic amygdaloidal texture and consists of phenocrystals of quartz, calcic oligoclase ( $An_{22,25}$ ), pyroxene and amphibole in a trachytic matrix.		
Iricoumé rhyolite/rhyodacite	The hornblende-rhyolite/rhyodacite consists of phenocrystals of feldspars, hornblende and Fe-Ti oxides in matrix of quartz, feldspars and hornblende. Small clusters of hornblende form radial arrangement. Two phenocrystals types of plagioclase. 1-type is subhedral-euhedral (1–2 mm), and has calcic oligoclase ( $An_{39}$ ) in composition. The plagioclase-2 (< 0.5 mm) is euhedral, has $An_{36}$ in composition. The alkali feldspar (1–2 mm) phenocrystal is subhedral and contains inclusions of plagioclase-2. The bulbous-type myrmekite is very frequent.		
Microgranite porphyry dike			The porphyritic texture containing feldspars crystals of up to 2 cm, medium- to fine-grained matrix and localized granophyric intergrowths.
Hornfels			Into the NE sector, mafic rocks and granitoids, above all, Canoas Syenogranite, were statically recrystallized. Present interlobate granoblastic texture and less recrystallized rocks possess igneous locally preserved texture, where is possible describe fibrous veins, crystalplastic deformation of quartz and fragile deformation of feldspars.

both being slightly following the magmatic flow. The quartz is usually anhedral and occurs as phenocrystals, as strings in amygdaloid rims and partially filling amygdaloids. The euhedral calcic oligoclase displays twinning according to the Albite-Carlsbad law. The pyroxene is scattered and is commonly associated with andesine and Fe-Ti oxides. The actinolite-tremolite, generated from the alteration of hornblende, is as fibrous crystals filling amygdaloids.

The hornblende rhyolite/rhyodacite consists of phenocrystals of feldspars, hornblende and Fe-Ti oxides in a matrix of quartz, feldspars and hornblende. Zircon and apatite are the most common accessory minerals. The hornblende phenocrystals are sub-hedral and commonly associated with the Fe-Ti oxides. They present inclusions of Fe-Ti oxides, and their contacts with the matrix are gradual. Clusters of small hornblende crystals in radial arrangements are common.

Two types of plagioclase phenocrystals have been recorded. Plagioclase-1 is sub-hedral-euhedral (from 1 to 2 mm) and has a calcic oligoclase ( $An_{29}$ ) composition. Plagioclase-2 (< 0.5 mm) is euhedral, has  $An_{26}$  composition, and also occurs as inclusion in the alkali feldspar. Both types of plagioclase exhibit Albite and Albite-Carlsbad law twinning. Their calcic cores break up into muscovite, sericite, and clay minerals.

The alkali feldspar phenocrystals (from 1 to 2 mm) are sub-hedral with inclusions of plagioclase-2. The bulbous-type myrmekite is very common and mainly occurs in the rims of larger crystals. Feldspars show strong wavy extinction and deformation lamellae. Such aspects are only observed in the phenocrystals and are absent in the matrix components. This suggests synvolcanic deformation associated with the attrition of crystals at the eruption vent, which only affected the phenocrystals that had already been formed. Among some feldspar crystals, there are clusters of intermediate size quartz-feldspar between the matrix and the phenocrystals. Some of the crystals in the clusters have the same optical orientation as the phenocrystals (Fig. 5C), which indicate the variations of mineral nucleation and growth rates involved in the formation of these volcanic rocks.

**Canoas Syenogranite** The hornblende-bearing syenogranites and minor hornblende-bearing alkali feldspar granites have a medium-grained seriate texture (Tab. 1, Fig. 4B). The alkali feldspar is sub-hedral and strongly perthitic (stringlets, strings, interlocking and chessboard albite) with generation of sub-hedral

albite crystals. It contains plagioclase inclusions, and its contacts with the plagioclase and quartz are faintly interdigitated. The euhedral, normal-zoned plagioclase measures between 0.5 and 3.0 mm. It is a sodic oligoclase ( $An_{10-12}$ ) and displays Albite and Albite-Carlsbad Law twinning. Its contacts with the alkali feldspar and quartz are rectilinear, and those with hornblende are interdigitated. The hornblende, strongly altered to chlorite, commonly occurs as interstitial crystals containing Fe-Ti oxide inclusions. The zircon is euhedral and measures up to 0.2 mm. Some sub-hedral titanite crystals have been greatly altered to epidote. According to geologist Desaix Silva (Brazilian Geological Service, personal communication), the garnet happens only in more evolved rocks as very fine crystals. The related mafic dikes are represented by quartz-gabbro and have intergranular and sub-ophitic textures, high amphibole contents, and plagioclase xenocrystals. The xenocrystals have been partially dissolved in their cores and rims.

**São Gabriel Granite** Hornblende monzogranite, hornblende syenogranite and biotite-hornblende syenogranite are the major petrographic variations observed in São Gabriel Granite (Tab. 1, Fig. 4C). Microgranite porphyry and microdiorite occur infrequently as dikes near the boundaries of the batholith. Medium-grained rapakivi-type textures predominate in all litho-types. Albite and Albite-Carlsbad Law twinning and major normal zoning, as well as minor abrupt and sectorial oscillatory zoning, are in two plagioclase types (Tab. 2).

Plagioclase-1 is euhedral (from 2 to 6.5 mm), has an  $An_{22}-An_{28}$  composition in the core (seen in different hydrothermal transformation zones) and an  $An_{22-17}$  one in the rims. The contacts are rectilinear with the hornblende-1 and are interpenetrative with the quartz-1. This plagioclase contains amphibole, Fe-Ti oxides, apatite, and zircon inclusions. The amphibole and Fe-Ti oxides inclusions are frequently located in the core of the plagioclase crystals. Plagioclase-1 and -2 form clusters similar to the Synneusis. Plagioclase-2 (0.5 – 1.5 mm) is anhedral-sub-hedral, unzoned and zoned (oscillatory). It is in the interstices between grains and contains inclusions of quartz-1 and biotite-2. In composition, it is  $An_{27-25}$  in the core and  $An_{21-17}$  in the rims. The alteration of the zoned plagioclase-2 resulted in anhedral crystals of epidote and sericite, whereas in the unzoned plagioclase-2, only sericite was formed.

Albite-Pericline law twinning is common in two alkali feldspar types. Manebach twinning is only observed in the alkali feldspar-2. The alkali feldspar-1 is sub-hedral (from 2.5 to 6 mm) and commonly occurs associated with quartz-1. The alkali feldspar-2 is sub-hedral-anhedral and measures 0.5 – 2.5 mm in length. Both alkali feldspars are slightly changed to sericite and clay minerals. Inclusions of plagioclase-2, hornblende-1, zircon, apatite, and perthite are very common. Albite microfilms grew along contacts and shift to a string-type arrangement coinciding with 001 cleavage. Locally interlocking and beaded perthites developed in the alkali feldspar-1 of the biotite-hornblende syenogranite. Intergranular albite is in all facies, however it is very abundant in the syenogranites. Some mantled alkali feldspar crystals (1-type) have ovoid shapes due to corroded rims (Fig. 5D). The product of alkali feldspar-1 exsolution seems to have grown on plagioclase-2 with corroded rims (anti-rapakivi-like) and on plagioclase-mantled alkali feldspar-1 (double mantle rapakivi-like).

Quartz-1 is anhedral-sub-hedral and measures 1 – 1.5 mm length. Quartz-2 is interstitial and is associated with biotite-2. Quartz-3 shows strong undulatory extinction and is typically precipitated on the alkali feldspar-1.

Hornblende-1 is sub-hedral to euhedral and is associated with Fe-Ti oxides and titanite. Alteration to chlorite is very common, but epidote and biotite are also observed. The contacts with the plagioclase-1 are rectilinear, whereas those with the quartz-1 and alkali feldspar-1 display re-entrances. The hornblende-1 has inclusions of Fe-Ti oxides. Hornblende-2 is associated with quartz-2 and fills interstices and cleavages of the plagioclase.

Sub-hedral crystals of biotite-1 display several apically corroded magnetite and ilmenite inclusions. The biotite-2 is a product of breaking-up hornblende-1 and -2, filling the interstices between grains.

The Fe-Ti oxides are coupled with hydrated Fe-Mg minerals and titanite. The latter happens as euhedral crystals up to 2 mm long and is associated with hornblende-1 and Fe-Ti oxides. Some titanite crystals have fluid inclusions with bubble shapes. The apatite is euhedral, acicular and hexagonal, and exhibits intimate relationships with hornblende-2 and plagioclases with simultaneous extinctions that suggest contemporaneous phases (Hibbard 1995). The zircon is euhedral to sub-hedral and sharply zoned.

The sericite-muscovite is associated with calcic portions of plagioclase. Low intensity argilization also occurred in the alkali feldspar. The epidote stands out by forming euhedral crystals, reflecting the high decalcification rates of calcic plagioclase. The albite is formed from the perthite. Hematite is common in alkali feldspar-rich granites. It is in sodic lamellas of perthite, interstitial among other minerals, filling microfractures, and as espherulitic crystals. Most of the hematite must have originated from magnetite-ilmenite alteration or substitution, precipitation on the feldspars by hydrothermal aqueous fluids.

The microgranite porphyry dikes contain feldspar crystals up to 2 cm in length (Fig. 5E), medium- to fine-grained matrix and local granophyric intergrowths, which mark the intrusive stage. The relationship between the phenocrystals and the matrix is similar to lava flow rhyolite, suggesting correlation.

The mingled microgranular enclaves (quartz-diorite, Fig. 5F) of São Gabriel Granite present textural and mineralogical features similar to those described for the mafic enclaves of Terra Preta Granite. Exceptions include the presence of biotite, amphibole pseudomorphs, and slightly more calcic plagioclases (An<sub>27-30</sub>).

**Crystallization sequences** The crystallization sequence of Terra Preta Granite (Fig. 6A) involves the stabilization of precocious minerals (apatite and zircon), followed by nucleation of plagioclase-1 (core) and stabilization of the Fe-Ti oxides. The high integrity of the oxides suggests slight participation in the formation of titanite. The synneusis relationship indicates that the plagioclase-2 grew concomitantly with some plagioclase-1 crystals. The presence of clinopyroxene pseudomorphs indicates a crystallization sequence, which includes deuteric reactions between varietal minerals and liquid.

The crystallization sequence of Canoas Syenogranite starts with the crystallization of zircon and apatite, followed by the consecutive crystallization of Fe-Ti oxides, plagioclase, quartz, hornblende, alkali feldspar, and titanite (Fig. 6B).

In São Gabriel Granite, the crystallization of the Fe-Ti oxides, Fe-Mg minerals, plagioclase, alkali feldspars and quartz were in a similar way as in the analyzed facies. The crystallization order (Fig. 6C) consisted of the stabilization of oxides, titanite, hornblende-1, biotite-1, plagioclase-1 core, apatite-zircon, plagioclase-1 rims, plagioclase-2 core, quartz-1,

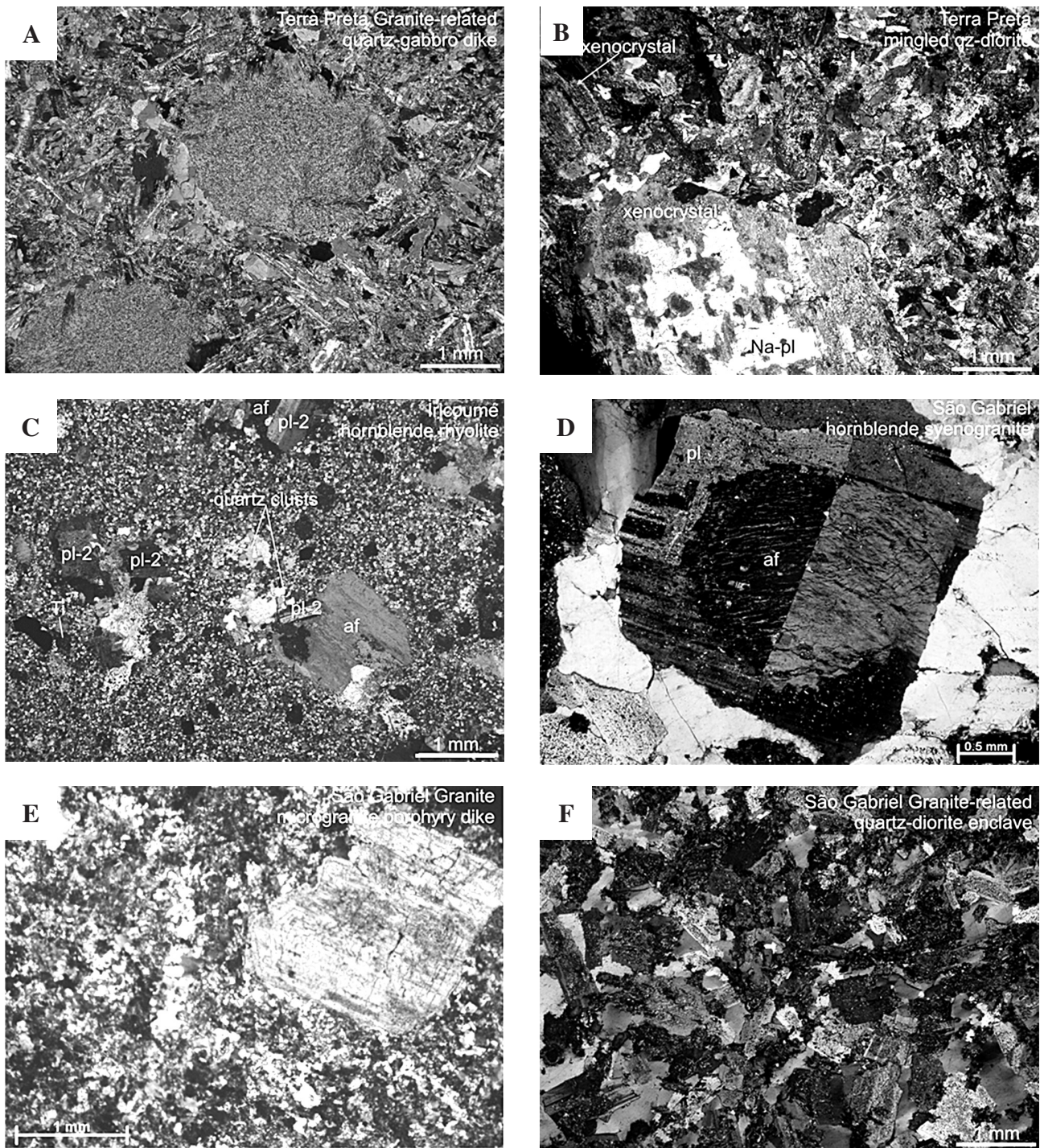


Figure 5 – Microtextural features of the studied plutons and related rocks. (A) Tremolite-actinolite and minor plagioclase in amygdaloidal structures in the Terra Preta Granite-related synplutonic quartz-gabbro. (B) Re-absorption features in xenocrystals of Terra Preta Granite hybrid quartz-diorite. (C) Intermediate-size crystal clusters between matrix and phenocrystals, displaying the same optical orientation as the phenocrystals. (D) Ovoid plagioclase mantled by perthitic alkali feldspars crystal (rapakivi texture). (E) Alkali feldspar crystal in microgranite porphyry dike. (F) Microgranular enclave of São Gabriel Granite. pl: plagioclase, af: alkali feldspar and qz: quartz.

and alkali feldspar-1. After the crystallization of the first phase, destabilization of the lower minerals temperature occurred, which resulted in the partial or total corrosion of the rims and congruent dissolution of the calcic core of the plagioclase-1 by forming plagioclase-3. The alkali feldspar-1 had their rims

corroded to form ovoid crystals, whereas part of the quartz-1 was solubilized. Stabilization of the crystals of hornblende-2 and quartz-2, alkali feldspar-2 and plagioclase-2 rims happened soon after. Some of the alkali feldspar-2 and plagioclase-2 appears to have only epitaxially grown on the plagioclases, corroded

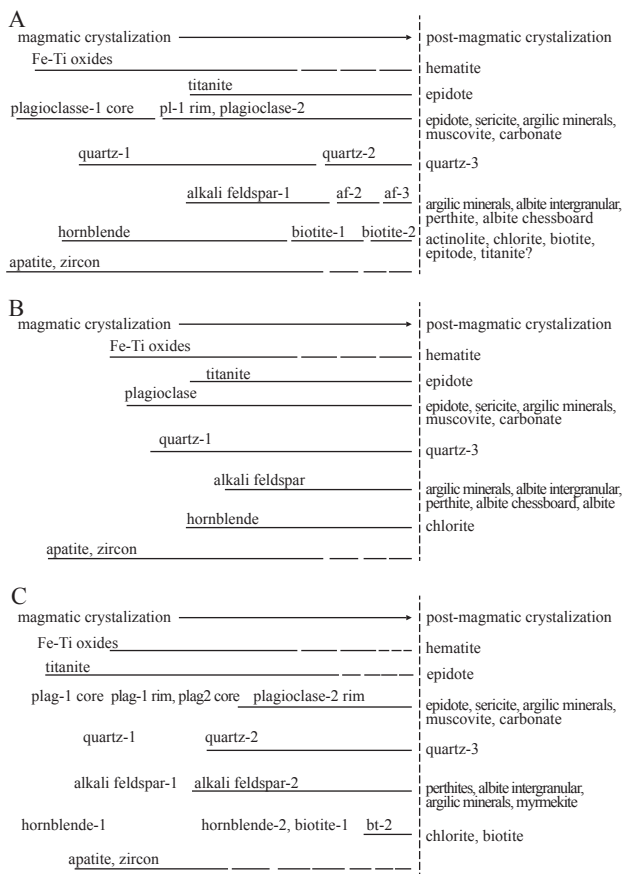


Figure 6 – Magmatic crystallization sequence and the postmagmatic minerals of Terra Preta Granite (A), Canoas Syenogranite (B), and São Gabriel Granite (C). The crystallization sequence was suggested from mineral inclusions and contacted relationships between crystals.

alkali feldspar rims, and the mantled alkali feldspar. These features are named *stricto sensu* anti-rapakivi and rapakivi and double-mantle rapakivi textures, respectively (Rämö 1991, Hibbard 1995, Rämö & Haapala 1995, Haapala & Rämö 1999).

**Dynamostatic rocks** The field and microdeformational features revealed increasingly intense deformation from E to W, recorded mainly in Terra Preta granitoids and minor Canoas syenogranites in the western sector of the study area. According to Paschier and Trouw's (1998) criteria, the deformed rocks registered low, low-medium, and medium-high temperatures.

The less deformed rocks have medium-grained granular texture. The quartz is ellipsoidal and moderately flattened, with rims that present undulatory extinction and sutured contacts. Mantles composed of small new-grains surround slightly deformed or undeformed porphyroclasts of quartz and feldspars. The quartz with strong undulatory extinction developed

deformation bands, whereas trails of neoblasts of quartz were formed in the boundaries of subgrains (Fig. 7A). The fragile structure of the alkali feldspar crystals allowed the local development of fractures filled by quartz, and it formed curved and rarely sigmoidal, antitaxial and fibrous quartz veins (Fig. 7B). The foliation is spaced and disjunctive and composes about 20% of the cleavage domain and 70% of the microlithes. The cleavage domain is irregular and its spatial relationship and transitions to the microlithe domains are anastomosed and gradual.

In the low-medium deformed rocks, recovery rate involves strong undulatory extinction and deformation bands and subgrains. Subgrain rotation is common and grain boundary migration is local. Some feldspar porphyroclasts have mantles of quartz neoblasts and trails, and fluid inclusions. Alkali feldspar porphyroclasts are surrounded by new grains of quartz and feldspar (mantle-core structure). Plagioclase inclusions, flame perthite and bulbous myrmekite rims are also common (Fig. 7C). The foliation is spaced, irregular disjunctive in about 30% of the cleavage domain, anastomosed, and gradual.

In the medium-high degree zone, the rocks are formed of a matrix of quartz and feldspars that are broadly recrystallized, in addition to quartz and feldspar porphyroclasts, biotite, and Fe-Ti-oxide trails. The quartz porphyroclasts occur as trail-shaped polycrystalline crystals due to accentuated stretching and formation/rotation of subgrains. Interdigitated subgrain contacts are associated with grain boundary migration of denser grains onto less dense ones. The feldspar porphyroclasts exhibit prominent mantle-core structure (Fig. 7D). The bulbous myrmekite is very common on alkali feldspars. Locally, the perthitic alkali feldspar displays antitaxial fibrous veins of quartz, suggesting that the pressure solution remained active during deformation. The alkali feldspar cores were preserved and myrmekites were formed on border-core boundaries. The foliation is spaced disjunctive, regular in about 80% of the cleavage domain and the contacts with microlithes are abrupt.

**Static metamorphic rocks** In the NE sector of the studied area, intermediate rocks and granitoids of São Gabriel Granite, and especially Canoas Syenogranite, have been statically recrystallized by a thermal event likely linked to intrusions of mafic dikes/stocks. The metagranites contain diabase dikes and pods displaying fractures that were filled by the

same material provided by one of the host rocks (Canoas Syenogranite).

**DIABASE** The recrystallized diabase (nematoblastic texture) displays schistose textures due to the emplacement structures (dikes) and spaced, disjunctive and irregular foliation with a cleavage domain of about 80% (Fig. 7E). It locally happens as lenses (*augen*) composed of actinolite inclusions in escapolite porphyroblasts. The *augen* seems to have been composed of amphibole, escapolite (meionite?) and epidote (clinzoisite) probably generated from pyroxene + H<sub>2</sub>O → hornblende and plagioclase + H<sub>2</sub>O → escapolite + epidote reactions. Hydrothermal reactions are observed in hornblende rims formed by actinolite. Escapolite occurs as < 0.1 mm crystals and 3 to 5 mm plagioclase pseudomorphs. The sub-hedral–euhedral (up to 0.2 mm) epidote is usually associated with escapolite and actinolite.

**GRANITOIDS** The predominant texture of the recrystallized granitoids is interlobate granoblastic, ranging from seriate to equigranular. Minor recrystallized rocks locally preserve igneous textures, including fibrous veins, crystal-plastic deformation of quartz, and fragile deformation of feldspars (Fig. 7F). With the exception of mafic dikes, all rocks contain muscovite associated with deformation, which is more abundant in the rocks that have no preserved igneous textures. The muscovite may have been generated by the hydration reaction of alkali feldspar + H<sub>2</sub>O → muscovite + quartz. The granolepidoblastic texture of Canoas muscovite hornfels xenoliths contrast with the equigranular interlobate granoblastic texture of São Gabriel Granite wall rock. This occurs by virtue of the decreasing thermal contrast between the partially assimilated wall rock fragments (sub-angular) and the host magma, preserving previous characteristics of a dynamo-thermal deformation event. These features and the presence of a dynamo-thermal event suggest a different deformational event between 1.88 Ga and younger mafic intrusions. Alternatively, the textural orientation of the enclaves may have happened due to increasing turbulent flux near the borders of São Gabriel magma chamber.

## DISCUSSION

**Lithostratigraphic units** The main 1.90 to 1.89 Ga calc-alkaline rocks of the central portion of Amazonian Craton are associated with Água

Branca Suite (CPRM 2006, Ferron 2006, Almeida 2006, Valério *et al.* 2006b). The more thoroughly studied pluton (Caroebe Granite) consists of a granitoid association of Peru- or Sierra Nevada-type granodiorite of the calc-alkaline series (Almeida 2006, Almeida & Macambira 2007). The Terra Preta Granite is classified in this study as an I-type, high-K calc-alkaline pluton, whose size and shape remain undefined due to reworking of its western and southern borders caused by a poorly defined deformational event and the cover of the Amazon basin (Valério *et al.* 2009 & 2010).

The Jauaperi Complex term was applied by CPRM (2006) to characterize gneiss and metagranites occurring in the southern region of the Guyana Shield. Our study showed that this region is dominated by Água Branca group and Mapuera granitoids and undivided mafic rocks, which recorded the effects of a supposed regional metamorphism whose age, amplitude, and magnitude were not delimited.

Based on their geochemical signatures and plutonic association types, the volcanic rocks from the NE Amazonas (1.89 – 1.87 Ga) were classified into a high-K calc-alkaline group associated with Água Branca granitoids (Jatapu volcanics) and an alkaline potassic-type related to the Mapuera granites (Almeida 2006, CPRM 2006, Valério *et al.* 2006A & B, Ferron *et al.* 2006 & 2010, Almeida & Macambira 2007, Marques *et al.* 2007). Ferron *et al.* (2006) proposed separating the volcanic rocks of Iricoumé Group into formations, and argued that Pitinga Province's volcanism is associated with the generation of alkaline-K, high-Sr, A-type granites. Part of this volcano-plutonic event was developed from preserved caldera structures (Ferron *et al.* 2006, Souza *et al.* 2007). Due to the high erosion rates that are characteristic of the area near the northern border of the Amazon basin, the supposed caldera structure of the study region was only faintly preserved.

However, the structural features are similar to classic models of eroded calderas (cauldrons) without sedimentary events (Lipman 1984 & 1997, Cole *et al.* 2005, Acocella 2007), such as the presence of effusive andesite, explosive eruptions caused by under-pressure (Acocella 2007), and presence of several ignimbrite deposits, intrusions of autoclastic breccias and microgranite porphyry, and lava flow deposits (hornblende rhyolite/rhyodacite) associated with the postcollapse phase.

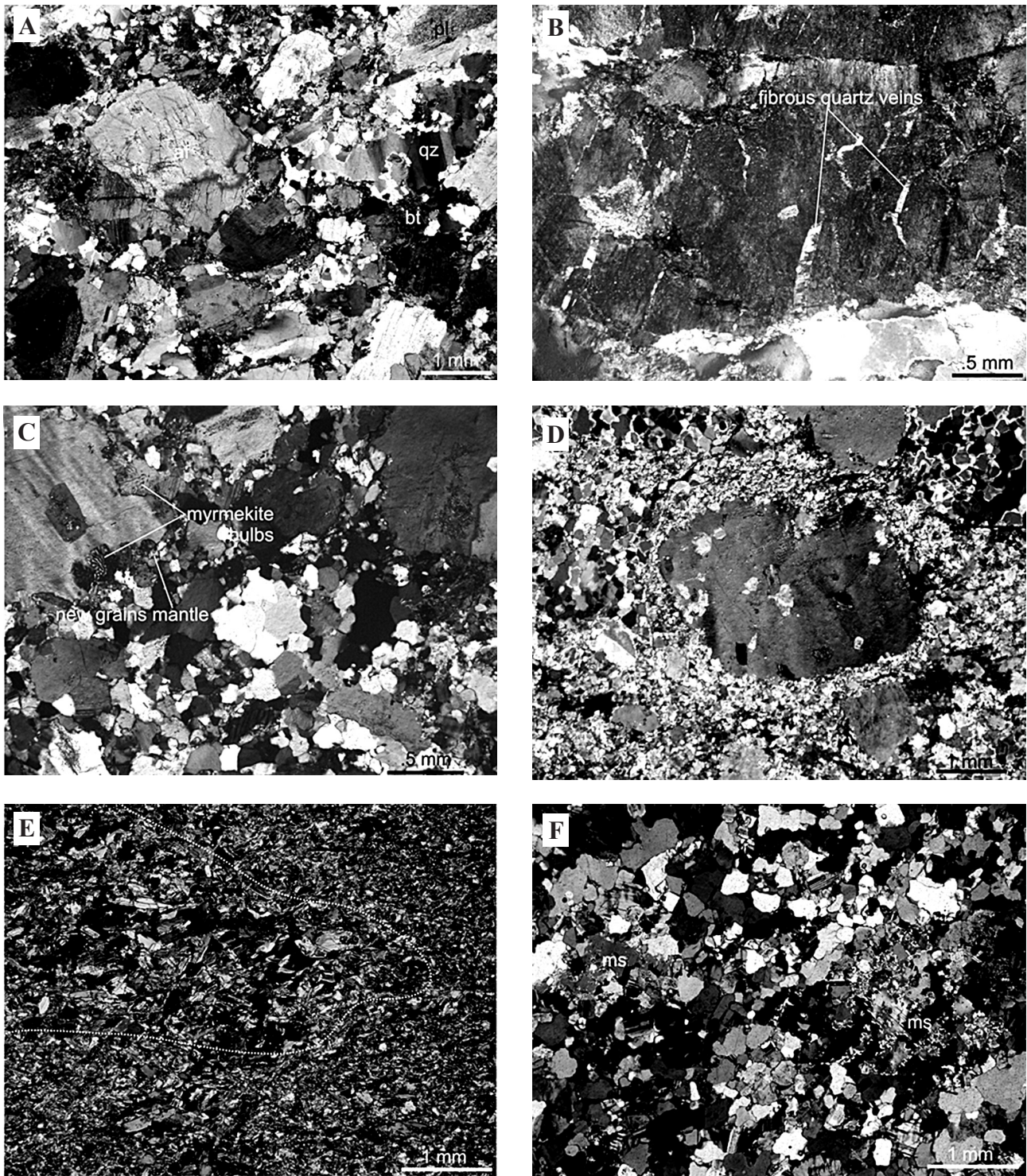


Figure 7 – Microtextural features of studied pluton-related metamorphic rocks. (A) Less deformed rocks of the study area. The quartz crystals present strong undulatory extinction and development of deformation bands, subgrains and trails of quartz neoblasts. (B) Antitaxial, fibrous quartz veins in fractured alkali feldspar crystals. (C) Rims of bulbous myrmekite and new grains on the plagioclase. (D) Prominent mantle-core structure in an alkali feldspar porphyroblast. (E) Detail of lenses composed of actinolite inclusions in an escapolite porphyroblast in diabase linked to statically recrystallized Canoas hornblende-bearing syenogranite (muscovite-actinolite hornfels). (F) Details of muscovite crystals in muscovite-actinolite hornfels. pl: plagioclase; af: alkali feldspar; qz: quartz; bt: biotite; ms: muscovite.

The Mapuera Suite is made up of several large A-type granite plutons emplaced at 1.89 to 1.86 Ga (CPRM 2006, Almeida 2006). Several stocks

of reddish syenogranites and minor alkali feldspar-granite associations were generically grouped into the Mapuera Suite, mainly based on geochemistry

and absolute ages, but without taking into consideration problems such as geochemical convergence and absence of field evidence. Valério *et al.* (2006a) showed that there are petrographic and geochemical similarities between biotite-hornblende syenogranite from the south/southeastern borders of São Gabriel Granite and other large granitic bodies of the Mapuera Suite, however this is not conclusive for Canoas Syenogranite. In addition, the major relationship of Canoas Syenogranite with Terra Preta granitoids has driven to classify some of these syenogranitic bodies as the São Gabriel Granite. Another aspect that supports this stratigraphic arrangement is the textural dissimilarity between the hornfels xenoliths (granolepidoblastic) and São Gabriel Granite wall rock (granoblastic).

Some of the mafic rocks from the southwest sector of the study area, described along the Pardo River (e.g., olivine-gabbro), have been included in the Seringa Formation, with 1.20 to 1.07 Ga (CPRM 2000). According to its original definition (Veiga Jr. *et al.* 1979), the Seringa Formation is characterized by mafic dikes and lava flow deposits. Differentiated diorites and quartz-diorites, not associated with calcic-alkaline granitoids, are only mentioned in the Quarenta Ilhas Formation (1.79 Ga) (CPRM 2006) and are never cited as rocks related to the studied granitoids.

**Petrological considerations** In the central-southern Guyana Shield (SE Roraima State, Brazil), Almeida *et al.* (2002) and Almeida & Macambira (2003) described important field and petrographic features that demonstrated the evolutionary processes of Água Branca magma, including the local assimilation of wall rocks. Ague & Brimhall (1987) observed similar aspects in calc-alkaline granitoids from Sierra Nevada. They showed that granitoid magmas were variably contaminated at regional and local scales by crustal igneous, metamorphic and sedimentary rocks. Chappell (1996) concluded that the assimilation processes and hybridization between mafic and felsic magmas do not result in great compositional variations and argued that the partial melting of the lower crust alone would explain such variations. Other authors have proposed that homogeneous petrographic types of granitoids could be formed by hybridization of crustal liquids with mafic magma (Frost & Mahood 1987, Huppert & Sparks 1988, Rämö 1991, Haapala & Rämö 1992

& 1999, Rämö & Haapala 1995) or with dioritic and tonalitic magmas derived, by fractional crystallization, from mantle basaltic liquids (Castro *et al.* 1990 & 1991).

Based only on the F, Zr, Nb and rare earth elements contents of the Mapuera magma, Ferron *et al.* (2010) advocated a mantle origin before being modified by subduction in a post-collision tectonic setting. However, they have also considered a bimodal origin in an extensional environment, as previously argued by Almeida (2006).

The present evaluation, based on field and petrographic data, suggest that, in addition to fractional crystallization, processes of wall rock assimilation and magma mingling had played a role, at least at the local scale, in the evolution of granitoids from the NE Amazonas State.

#### **Texture and deformation of Terra Preta and Canoas granitoids**

Barker (1970) showed that granophyric intergrowths could be formed in response to the simultaneous/rapid crystallization of alkali feldspar and quartz from liquid or vapor. The origin of intergrowths would involve volatile-rich liquids in the final processes of crystallization in epizonal environments (Hibbard 1979, & 1987, Hughes 1982). These magmatic conditions are compatible with underformed granitoids with restricted granophyric textures that are likely related to the presence of aplite dikes formed from sudden replacement of H<sub>2</sub>O-saturated phases, due to pressure loss that accelerated the nucleation rates (Hibbard 1995). In recrystallized granitoids, however, the granophyric textures must be associated with dynamo-thermal deformation.

The bulbous and intergranular myrmekites that were developed along alkali feldspar boundaries showed different crystallographic orientations. For Phillips (1974, 1980), and Smith & Brown (1988), the myrmekite is formed by the exsolution of alkali feldspar accompanied of pressure-induced dissolution and reprecipitation in a *subsolvus* state with some participation of primary quartz and K-feldspar. Smith & Brown (1988) suggested that subsequent processes could partially or completely modify the myrmekite by recrystallizing it. This points out myrmekites as petrogenetic indicators and suggests that myrmekites in the dynamically crystallized studied granitoids must have been originated from *subsolvus* deformational processes.

The origin theories of the deformation process proposed for rocks of the area study are controversial, not only due to limited geochronological data, but also because of the incomplete knowledge of structural features at the field level. The reconstitution of events shows that Terra Preta Granite was emplaced during the postcollisional uplift, followed by deformation induced by the effects of oceanic plate subduction under the Vantuari-Tapajós paleocontinent at the beginning of Rio Negro Province building (Valério *et al.* 2009). This model can be valid if we consider the different crustal levels between the undeformed São Gabriel Granite (and related rock) and Terra Preta Granite and Canoas Syenogranite (deformed). In contrast, CPRM (2000) and Valério *et al.* (2006b) presented a collisional model that is incompatible with the small difference in age (~ 10 Ma) and petrographic dissimilarities between the syncollisional and anorogenic bodies. Therefore, based on petrographic analysis, it is simpler to think that this deformation and metamorphism must be linked to an event slightly younger than the Terra Preta magmatism, which was likely associated with strike-slip faults in an extensional setting, whose effects were not registered by the subvolcanic, shallower São Gabriel Granite and related rocks.

**CONCLUSION REMARKS** Field and petrographic features supported by previous works raised in this study lead to the following conclusions:

- Transitional contact zones between partially fragmented mafic dikes and wall rocks (Terra Preta hornblende granodiorite), where mafic and intermediate enclaves with low and high xenocrystals contents, respectively, and mingled quartz-diorite, have been formed. These features indicate that at least one generation of mafic dikes was emplaced before the complete crystallization of Terra Preta Granite.
- The diffuse contact and recrystallized xenoliths suggests that Canoas Syenogranite is slightly younger than Terra Preta Granite and older than São Gabriel Granite. We considered that the Canoas hornblende-bearing syenogranites were generated from Mapuera magma. However, the intimate field relationships with the Terra Preta granitoids and differentiated mineral paragenesis point to a divergent

evolution, and therefore its association with Mapuera magma is not conclusive.

- Interaction features and petrographic evidence suggest that, in addition to fractional crystallization, assimilation and magma mingling processes played a role at least in the local scale, in the evolution of the Terra Preta Granite, Canoas Syenogranite and São Gabriel Granite. Microfeatures of magma mingling have been found in all granitoid plutons at variable rates, such as plagioclase dissolution, feldspar rim corrosion, alkali feldspar and plagioclase mantles, a second generation of apatite and high xenocrystals contents in mafic enclaves.
- The crystallization sequences support fractional crystallization as a dominant differentiation process of Terra Preta Granite and Canoas Syenogranite, while in São Gabriel Granite, magma mingling seems to have been in harmony with all phases of fractional crystallization.
- Undeformed gabbros, diorites and minor anorthosite likely are linked to the rapakivi-type São Gabriel Granite. Except near these undeformed rocks, all granitoids in the western sector of the study area recorded appreciable and progressive dynamostatic deformation from E to W. Such event must have occurred between 1.90 Ga (Terra Preta Granite) and the intrusions of the São Gabriel Granite (1.89 Ga) and related rocks. We point to an alternative origin, which is associated with an event slightly younger than the postcollisional uplift. However, it is extremely necessary to obtain absolute ages for this metamorphic event, which is the purpose of these authors' next paper.

**ACKNOWLEDGEMENTS** This research was financed by the Institute of Geosciences, Federal University of Pará and the CT-Amazonia project (MCT-CNPq 575520/2008-6). We thank the Brazilian National Council of Technological and Scientific Development (CNPq) scholarship (140758/2007-0) granted for funding the first author, and the Department of Geosciences, Federal University of Amazonas, for storing the samples gathered in the field and for partial sample preparation.

## References

- Acocella V. 2007. Understanding caldera structure and development: An overview of analogue models compared to natural calderas. *Earth-Science Reviews*, **85**:125-160.
- Ague J.J. & Brimhall G.H. 1987. Granites of batholiths of California: Products of local assimilation and regional-scale crustal contamination. *Geology*, **15**:63-66.
- Almeida M.E. 2006. *Evolução geológica da porção centro-sul do escudo das Guianas com base no estudo geoquímico, geocronológico (evaporação de Pb e U-Pb ID-TIMS em zircão) e isotópico (Nd-Pb) dos granitóides Paleoproterozóicos do sudeste de Roraima*. Tese de Doutorado, Programa de Pós-Graduação em Geologia e Geoquímica, Instituto de Geociências, Universidade Federal do Pará, Belém, 227 p. (in portuguese).
- Almeida M.E., Macambira M.J.B., Faria MSG. 2002. A Granitogênese paleoproterozóica do sul de Roraima. In: SBG, Congresso Brasileiro de Geologia, 41, *Anais*, p. 434. (in portuguese).
- Almeida M.E. & Macambira M.J.B. 2003. Aspectos geológicos e litoquímicos dos granitóides cálcio-alcálicos Paleoproterozóicos do sudeste de Roraima. In: SBGq, Congresso Brasileiro de Geoquímica, 9, *Anais*, p. 775-778. (in portuguese).
- Almeida M.E. & Macambira M.J.B. 2007. Geology and petrography of the paleoproterozoic granitoid rocks from Uatumã-Anauá domain, central region of Guyana Shield, southeastern Roraima, Brazil. *Revista Brasileira de Geologia*, **37**(1):2-21.
- Almeida M.E., Macambira M.J.B., Oliveira E.C. 2007. Geochemistry and zircon geochronology of the I-type high-K calc-alkaline and S-type granitoid rocks from southeastern Roraima, Brazil: Orosirian collisional magmatism evidence (1.97–1.96 Ga) in central portion of Guyana Shield. *Precambrian Research*, **155**(1-2):69-97.
- Almeida M.E., Macambira M.J.B., Valente S.C. 2008. New geological and single-zircon Pb evaporation data from the Central Guyana Domain, southeastern Roraima, Brazil: Tectonic implications. *Journal of South American Earth Sciences*, **26**:318-328.
- Araújo Neto H. & Moreira H.L. 1976. Projeto Estanho de Abonari. Brasília, Ministério de Minas e Energia, Departamento Nacional de Produção Mineral, Companhia de Pesquisa e Recursos Minerais (MME/DNPM/CPRM), *Relatório*, 1:232. (in portuguese).
- Barker D.S. 1970. Composition of granophyre, myrmekite, and graphic granite. *Geological Society of America Bulletin*, **81**:3339-3350.
- Bull K.F. & McPhie J. 2007. Fiamme textures in volcanic successions: Flaming issues of definition and interpretation. *Journal of Volcanology and Geothermal Research*, **164**:205-216.
- Campbell L.H. 1996. Fluid dynamic process in basaltic magma chamber. In: Cawthorn R.G. (ed). *Layered intrusions* (Developments in Petrology). Elsevier Science, London, 519 p.
- Castro A., De la Rosa J.D., Stephen W.E. 1990. Magma mixing in the subvolcanic environment: petrology of the Genera interaction zone near Seville, Spain. *Contributions to Mineralogy and Petrology*, **105**:9-26.
- Castro A., Moreno-Ventas I., De la Rosa J.D. 1991. H-type (hybrid) granitoids: a proposed revision of the granite-type classification and nomenclature. *Earth-Science Reviews*, **31**:237-253.
- Chappel B.W. 1996. Magma mixing and the production of compositional variation within granite suites: evidence from the granites of southeastern Australia. *Journal of Petrology*, **37**(3):449-470.
- Cole J.W., Milner D.M., Spinks K.D. 2005. Calderas and caldera structures: a review. *Earth-Science Reviews*, **69**:1-96.
- Costi H.T., Santiago A.F., Pinheiro S.S. 1984. Projeto Uatumã-Jatapu, *Relatório Final*. Manaus: CPRM – SUREG-MA. 133 p. (in portuguese).
- Costi, H.T., Dall’Agnol, R., Moura, C.A.V. 2000. Geology and Pb-Pb geochronology of Paleoproterozoic volcanic and granitic rocks of the Pitinga Province, northern Brazil. *International Geology Reviews*, **42**:832-849.
- Costi H.T., Valério C.S., Alves M.A.S., Souza V.S. 2009. *Overview of the geology of southernmost Guyana Shield, Presidente Figueiredo district, NE Amazonas: Guide and field trip program*. In: SBG-Núcleo Norte, Simpósio de Geologia na Amazônia, 11, Manaus (AM), CD-Rom.
- CPRM – Serviço Geológico do Brasil. 2000. *Programa Levantamentos Geológicos Básicos do Brasil. Caracará, Folhas NA.20-Z-B e NA.20-Z-D inteiras e parte das folhas NA.20-Z-A, NA.20-Z-C, NA.21-Y-C e NA.21-Y-A*. Estado de Roraima. Escala 1:500.000. Brasília, CD-Rom. (in portuguese).
- CPRM – Serviço Geológico do Brasil. 2006. *Geologia e recursos minerais do estado do Amazonas*. Escala 1:1.000.000, CPRM/CIAMA, Manaus, 180 p. (in portuguese).
- Faria, M.S.G., Santos, J.O.S., Luzardo, R., Hartmann, L.A., 2002. *The oldest Island Arc of Roraima state, Brazil – 2.03Ga: Zircon Shrimp U–Pb geochronology of Anauá Complex*. In: SBG, Congresso Brasileiro de Geologia, vol. 41. João Pessoa, PB, *Anais*, p. 38.
- Faria M.S.G., Almeida M.E., Santos J.O.S., Chemale Jr. F. 2003. *Evolução geológica da região do alto Rio Anauá - Roraima*. In: SBG-Núcleo Norte, Simpósio de Geologia no Amazonas, 8, Manaus (AM), CD-Rom. (in portuguese).
- Ferron J.M.T.M. 2006. *Geologia regional, geoquímica, geocronologia Pb-Pb de rochas graníticas e vulcânicas paleoproterozóicas as Província Pitinga, Cráton Amazônico*. Tese de Doutorado, Programa de Pós-Graduação Geociências, Universidade Federal do Rio Grande do Sul, Porto Alegre, 331 p. (in portuguese).

- Ferron J.M.T.M., Bastos Neto A.C., Lima E.F., Costi H.T., Moura C.A.V., Prado M., Pierosan R., Galarza M.A. 2006. Geologia e geocronologia Pb-Pb de rochas graníticas e vulcânicas ácidas a intermediárias paleoproterozóicas da Província Pitinga, Cráton Amazônico. *Revista Brasileira de Geociências*, **36**(3):499-512. (in portuguese).
- Ferron J.M.T.M., Bastos Neto A.C., Lima E.F., Nardi L.V.S., Costi H.T., Pierosan R., Prado M. 2010. Petrology, Geochemistry, and Geochronology of Paleoproterozoic Volcanic and Granitic Rocks (1.89 to 1.88 Ga) of the Pitinga Province, Amazonian Craton, Brazil. *Journal of South American Earth Sciences*, **29**:483-497.
- Freitas M.E., Chagas A.N.B., Araújo F.M., Mejia N.I.M. 2007. *Interpretação das texturas das rochas vulcânicas do Grupo Iricoumé na região de Presidente Figueiredo – AM*. In: SBG-Núcleo Norte, Simpósio de Geologia no Amazonas, 10, Porto Velho (RO), CD-Rom. (in portuguese).
- Frost T.P. & Mahood G.A. 1987. Field, chemical, and physical constraints on mafic-felsic magma interaction in the Lamarck granodiorite, Sierra Nevada, California. *Geological Society of America Bulletin*, **99**:272-291.
- Haapala I. & Rämö O.T. 1992. Tectonic setting and origin of The Proterozoic rapakivi granites of southeastern Fennoscandia. *Transactions of the Royal Society of Edinburgh: Earth and Environmental Science*, **83**:165-171.
- Haapala I. & Rämö O.T. 1999. Rapakivi granites and related rocks: an introduction. *Precambrian Research*, **95**:1-7.
- Hibbard M.J. 1979. Myrmekite as a marker between pre and post aqueous phase saturation in granitic systems. *Geological Society of America Bulletin*, **90**:1047-1062.
- Hibbard M.J. 1987. Deformation of incompletely crystallized magma systems: granite gneisses and their tectonic implication. *Journal of Geology*, **95**:543-561.
- Hibbard M.J. 1995. *Petrography to petrogenesis*. Prentice Hall Inc., New Jersey, USA, 587 p.
- Hughes C.J. 1982. *Igneous Petrology*. Elsevier Science, New York, Developments in Petrology, 7, 551 p.
- Huppert H.E. & Sparks R.S.J. 1988. The generation of granitic magma by intrusion of basalt into continental crust. *Journal of Petrology*, **29**:599-624.
- Lameyre J. & Bowden P. 1982. Plutonic rocks type series: discrimination of various granitoid series and related rocks. *Journal of Volcanology and Geothermal Research*, **14**:169-186.
- Lipman P.W. 1984. The roots of ash flow calderas in Western North America: windows into the tops of granitic batholiths. *Journal of Geophysical Research*, **89**:8801-8841.
- Lipman P.W. 1997. Subsidence of ash-flow calderas: relation to caldera size and magma-chamber geometry. *Bulletin of Volcanology*, **59**:198-218.
- Macambira M.J.B., Vasquez M.L., Silva D.C.C., Galarza M.A., Barros C.E.M., Camelo J.F. 2009. Crustal growth of the central-eastern Paleoproterozoic domain, SE Amazonian craton: Juvenile accretion vs. reworking. *Journal of South American Earth Science*, **27**:235-246.
- Marques S.N.S., Nascimento R.S.C., Souza V.S., Dantas E.L. 2007. *Características geoquímicas das rochas vulcânicas do Grupo Iricoumé, em perfis estratigráficos, na região de Presidente Figueiredo-AM*. In: SBG-Núcleo Norte, Simpósio de Geologia no Amazonas, 10, Porto Velho-RO, CD-Rom. (in portuguese).
- Paschier C.W. & Trouw R.A.J. 1998. *Microtectonics*. Springer, CD-Rom.
- Phillips E.R. 1974. Myrmekite – one hundred years later. *Lithos*, **7**:181-194.
- Phillips E.R. 1980. On polygenetic myrmekite. *Geological Magazine*, **117**:29-36.
- Rämö O.T. 1991. Petrogenesis of the Proterozoic rapakivi granites and related basic rocks of southeastern Fennoscandia: Nd and Pb isotopic and general geochemical constraints. *Geological Survey of Finland Bulletin*, **355**, 161 p.
- Rämö O.T. & Haapala I. 1995. One hundred years of rapakivi granite. *Mineralogy and Petrology*, **52**:129-185.
- Santos J.O.S., Moreira A.S., Pessoa M.R., Oliveira J.R., Malouf R.F., Veiga Jr. J.P., Nascimento J.O. 1974. Projeto Norte da Amazônia, domínio baixo Rio Negro. DNPM/CPRM, *Relatório Final Integrado*, Manaus, Vol. 4. (in portuguese).
- Santos J.O.S., Silva L.C., Faria M.S.G., Macambira M.J.B. 1997. *Pb-Pb single crystal, evaporation isotopic study on the post-tectonic, subalkalic, A-type Moderna granite (Mapuera Intrusive Suite), State of Roraima, northern Brazil*. In: International Symposium on granites and related mineralizations. Salvador, Extended Abstracts, 1:273-275.
- Santos J.O.S., Faria M.S.G., Hartmann L.A., McNaughton N.J., Fletcher I.R. 2001. *Oldest charnockite magmatism in the Amazon craton: zircon U-Pb SHRIMP geochronology of the Jaburu Charnockite, Southern Roraima, Brazil*. In: SBG/NO, Simpósio de Geologia da Amazônia, 7, Belém, *Workshop II*, 4 p.
- Santos J.O.S., Hartmann L.A., Faria M.S.G., Riker S.R.L., Souza M.M., Almeida M.E., McNaughton N.J. 2006. *A compartimentação do Cráton Amazonas em províncias: avanços ocorridos no período de 2000–2006*. In: SBG-NO, Simpósio de Geologia da Amazônia, 9, Belém, CD-Rom. (in portuguese).
- Smith J.V. & Brown W.L. 1988. *Feldspar minerals: crystals structures, physical, chemistry and textural properties*. Springer Verlag, Berlin, **2**, 2ed. 828 p.
- Souza A.G.H., Milliotti C.A., Luzardo R. 2006. *Caracterização petrográfica das rochas aflorantes na pedreira do Getúlio, região de Presidente Figueiredo (AM)*. In: SBG, Congresso Brasileiro de Geologia, 43, CD-Rom. (in portuguese).
- Souza V.S., Marques S.N.S., Nascimento R.S., Valério C.S. 2007. *Texturas e estruturas em rochas piroclásticas e vulcânicas paleoproterozóicas do Grupo Iricoumé, sudeste do Município de Presidente Figueiredo (AM)*. In: SBG-NO, Simpósio de Geologia no Amazonas, 10, Porto Velho-RO, CD-Rom. (in portuguese).

- Souza V.S. & Nogueira A.C.R. 2009. Seção geológica Manaus–Presidente Figueiredo (AM), borda norte da Bacia do Amazonas: Um guia para excursão de campo. *Revista Brasileira de Geociências*, **39**(1):16-19. (in portuguese).
- Streckeisen A. 1976. To each plutonic rock its proper name. *Earth-Sciences Reviews*, **12**:1-33.
- Tassinari C.C.G., Macambira M.J.B. 1999. Geochronological provinces of the Amazonian Craton. *Episodes*, **22**(3):174-182.
- Tassinari, C.C.G., Bettencourt, J.S., Geraldés, M.C., Macambira, M.J.B., Lafon, J.M., 2000. The Amazonian Craton. In: UG Cordani, EJ Milani, A Thomaz Filho, DA Campos (Edit.). Tectonic Evolution of South America. 31<sup>st</sup> International Geological Congress, Rio de Janeiro, Brazil, p.41–95.
- Tassinari, C.C.G. & Macambira, M.J.B. 2004. A evolução tectônica do cráton Amazônico. In: V. Mantesso-Neto, A. Bartorelli, C. Dal Ré Carneiro, B.B. Brito-Neves. Geologia do Continente Sul-Americano: Evolução da obra de Fernando Flávio Marques de Almeida. Beca, São Paulo, p.471–485 (in portuguese).
- Valério C.S., Souza V.S., Macambira M.J.B., Milliotti C.A, Carvalho A.S. 2005. Geoquímica e idade Pb-Pb de zircão do Grupo Iricoumé na região da borda norte da bacia do Amazonas, município de Presidente Figueiredo (AM). In: SBG, Simpósio de Vulcanismo e Ambientes Associados, 3, p. 47-52. (in portuguese).
- Valério C.S. 2006. *Magmatismo Paleoproterozóico do extremo sul do Escudo das Guianas, município de Presidente Figueiredo (AM): geologia, geoquímica e geocronologia Pb-Pb em zircão*. Dissertação de Mestrado, Departamento de Geologia, Programa de Pós-graduação em Geociências, Universidade Federal do Amazonas, Manaus, 112 p. (in portuguese).
- Valério C.S., Souza V.S., Macambira M.J.B., Galarza M.A. 2006A. Aspectos geoquímicos e idade Pb-Pb da borda sudeste do batólito São Gabriel, Município de Presidente Figueiredo (AM), Escudo das Guianas: Implicações tectônicas. In: SBG/NO, Simpósio de Geologia no Amazonas, 9. CD-Rom (in portuguese).
- Valério C.S., Souza V.S., Macambira M.J.B., Galarza M.A. 2006B. Geoquímica e geocronologia Pb-Pb da Suíte Intrusiva Água Branca, Município de Presidente Figueiredo (AM): evidências de colisão no Paleoproterozóico da Amazônia Ocidental. *Revista Brasileira de Geociências*, **36**(2):359-370. (in portuguese).
- Valério C.S., Souza V.S., Macambira M.J.B. 2009. The 1.90–1.88 Ga magmatism in the southernmost Guyana Shield, Amazonas, Brazil: geology, geochemistry, zircon geochronology, and tectonic implications. *Journal of South American Earth Sciences*, **28**(3):304-320.
- Valério C.S., Macambira M.J.B., Souza V.S. 2010. *Litoestratigrafia e aspectos petrogenéticos de granitóides tipos I e A (1,90–1,88 Ga) do SW do município de Presidente Figueiredo, NE do Amazonas*. In: SBG, Congresso Brasileiro de Geologia, 45, Belém, CD-Rom. (in portuguese).
- Veiga Jr. J.P., Nunes A.C.B., Souza E.C., Santos J.O.S., Amaral J.E., Pessoa M.R., Souza S.A.S. 1979. *Projeto Sulfetos do Uatumã*. Manaus, DNPM/CPRM. Relatório Final, vol.6. (in portuguese).

**Manuscrito ID 21782**

**Recebido em: 27/06/2011**

**Aprovado em: 24/07/2012**